Food and Bioprocess Technology (2021) 14:2336–2346
https://doi.org/10.1007/s11947-021-02727-7

ORIGINAL RESEARCH

Sustainable Packaging Films Composed of Sodium Alginate and Hydrolyzed Collagen: Preparation and Characterization

Luís Marangoni Júnior[1] · Plínio Ribeiro Rodrigues[2] · Renan Garcia da Silva[1,2] · Roniérik Pioli Vieira[2] · Rosa Maria Vercelino Alves[1]

Received: 14 July 2021 / Accepted: 26 October 2021 / Published online: 4 November 2021

Abstract

Hydrolyzed collagen (HC) has been extensively explored in the food sector because of its functional properties and broad availability as a low-cost byproduct. However, its widespread use as a component of edible films lacks detailed information. In this study, sodium alginate/hydrolyzed collagen (SA/HC) films with distinct loadings of HC (10, 20, and 30%) were prepared. FT-IR results suggested the formation of intermolecular chemical bonds between SA and HC. When the control sample was compared with the highest concentration of HC evaluated, it was confirmed that incorporating HC increased the maximum degradation rate temperature from 226.51 to 232.89 °C (second thermal event). The thickness of all the SA/HC films increased as a function of the HC load, and a reduction of the water vapor transmission rate (WVTR) from 1215.7 ± 71.0 to 592.4 ± 52.2 g m^{-2} day^{-1} was observed. Although SEM images showed the addition of hydrolyzed collagen led to a discontinuity in the film polymeric matrix, there was no statistically significant influence on the tensile strength. However, the elongation at break experienced a significant reduction (from 11.1 ± 7.4 to 4.0 ± 2.4%), by comparing the control sample and a 30% HC loading. In general, SA/HC films with a 10% HC loading resulted in a superior general performance, so this formulation is recommended for future food packaging studies.

Keywords Biopolymer · Protein film · Polysaccharide film · Alginate

Introduction

The replacement of synthetic polymers by natural biopolymers remains an increasingly expanding topic in research aiming at a more sustainable environment (Berti et al., 2021; Ribeiro et al., 2021; Vianna et al., 2021; Zanela et al., 2021). Proteins and polysaccharides represent examples of outstanding renewable and biodegradable biopolymers for the production of edible films for food packaging (Khashayary & Aarabi, 2021; Marangoni Júnior et al., 2021a; Oliveira Filho et al., 2021; Silva Pereira et al., 2021). The formulation of blends of proteins and polysaccharides allows an attractive alternative for improving some physicochemical properties (Cazón et al., 2017; Gómez-Guillén et al., 2009; Jamróz et al., 2018), in addition to the possibility of obtaining films with functional activities (Gagliarini et al., 2019; Marangoni Júnior et al., 2020a; Motedayen et al., 2013). Among the various types of renewable polymers available, hydrolyzed collagen (HC) stands out because of its numerous functional activities and low cost. However, its potential has still been relatively little explored for biobased film production.

Obtained from native collagen sources (e.g., bovine, porcine, and marine), HC is a group of peptides produced by enzymatic action in an acid or alkaline environment (Garrido et al., 2019; León-López et al., 2019). While native collagen possesses an average molar mass ranging from 285 to 300 kDa, the HC average molar masses are remarkably low (3–6 kDa). It has been reported that compared with native collagen, HC has a lower viscosity, better water solubility, and sensorial properties (Denis et al., 2008; Zhang et al., 2006), which represent an advantage from the film processing perspective. In addition, HC retains a higher bioavailability than native collagen, and peptides resulting from its

✉ Luís Marangoni Júnior
marangoni.junior@hotmail.com

[1] Packaging Technology Center, Institute of Food Technology, Av. Brasil, Campinas, São Paulo 2880, 13070-178, Brazil

[2] Department of Bioprocess and Materials Engineering, School of Chemical Engineering, University of Campinas, Campinas, São Paulo, Brazil

ingestion offer chemotactic properties for skin fibroblasts, helping the skin restoration process. Therefore, HC has been widely employed as a food ingredient with defined physiological effects (nutraceuticals) (Gomez-Guillen et al., 2011; Ito et al., 2018; Lupu et al., 2020).

Moreover, HC can be obtained as a byproduct of animal processing in several industries. For example, fleshing, and shavings, made up mainly of raw collagen, represent the most significant solid waste in the tannery industry. Such byproducts are processed, and collagen hydrolysates in solution or powder are obtained. Therefore, HC is a low-cost material and its use in the bioplastics sector does not compete with the food industry, unlike starch or other protein sources (Seggiani et al., 2019). Despite possessing these advantages, HC does not form films by itself (Ramadass et al., 2014; Silvipriya et al., 2015). Hence, the incorporation of HC in the formulation of other biopolymer-based films can represent an easy strategy to take advantage of its functional properties, as well as lowering the cost of the final bioplastic products. Sodium alginate (SA) is a linear polysaccharide with a backbone of (1–4) linked β-d-mannuronic acid (M units) and α-l-guluronic acid (G units) (Mahmoud et al., 2020). SA is one of the most well-known polysaccharides with excellent film-forming ability, biodegradability, and non-toxicity that can be employed in the production of edible films (Marangoni Júnior et al., 2021b; Rahmani et al., 2017; Reyes-Avalos et al., 2016; Uyen et al., 2020; Venkatesan et al., 2015).

To the best of the author's knowledge, among the numerous biopolymers available for the formulation of blends with sodium alginate, hydrolyzed collagen has been unexplored until the present date. The fundamental hypothesis of this study was that adding HC would not harm the properties of SA-based films, allowing this component to be used more frequently in this regard. Thus, the aim of this study was to investigate the impact of including different proportions of HC on the physicochemical, optical, and morphological properties of SA-based films. The importance of this work lies in the fact that it will represent the first thorough description of the interactions between SA and HC for the production of edible films. Therefore, we believe this work may be the starting point in the expansion of studies evolving practical applications of hydrolyzed collagen as a food packaging material.

Materials and Methods

Material

The materials used in the preparation of the films were sodium alginate (SA), glycerol (Dinâmica Química Contemporânea Ltda, Indaiatuba/SP, Brazil), hydrolyzed collagen (HC) with 90% protein (NaturalLife, São José do Rio Preto/SP, Brazil), and distilled water.

Preparation of Film-Forming Solution and Films Samples

Sodium alginate and hydrolyzed collagen blended films (SA/HC) were prepared using the casting method. First, SA solutions (4% w/w) were prepared by dissolving the biopolymer in distilled water containing glycerol as a plasticizer (30% w/w based on the SA mass). Four film-forming solutions with different concentrations of HC were prepared (0, 10, 20, and 30% w/w based on the SA mass). The film-forming solution was heated to 80 °C with stirring for 20 min, then treated in an ultrasound bath for 15 min to ensure a homogeneous solution and elimination of bubbles. After this step, 40 g of film-forming solution were poured into polystyrene Petri dishes (14 cm diameter). The solutions were dried in a forced-air oven (Ethik Technology, Vargem Grande Paulista/SP, Brazil) at 40 °C for 20 h. The films were labeled as control samples SA, SA/HC10%, SA/HC20%, and SA/HC30%. All films were placed in an air-conditioned laboratory at 25 °C and 75% RH before the characterization test.

Characterization of SA/HC Films

Surface Morphology

The surface and cross-section (fractured with liquid nitrogen) microstructures of the film samples were visualized using a scanning electron microscope (SEM) (Leo 440i, LEO Electron Microscopy/Oxford, Cambridge, UK) at an acceleration voltage of 15 kV, 50 pA current, and magnification of 1000×. Before visualization, the film samples were fixed on a metallic support with the aid of double-sided carbon tape and covered with gold in a sputter coater (SC7620, VG Microtech, Kent, UK).

Fourier-Transform Infrared Spectroscopy (FT-IR)

The FT-IR spectra of the SA and SA/HC films were recorded using a Thermo Scientific spectrophotometer (Nicolet Continuum, Madison, WI, USA) in the wave number range between 4000 and 650 cm^{-1}, using the attenuated total reflectance module (ATR) with a resolution of 4 cm^{-1}.

Thermogravimetric Analysis (TGA)

The thermal analysis was conducted on a thermogravimetric analyzer (Mettler Toledo, TGA/DSC1, Schwerzenbach, Switzerland) and used to investigate the influence of HC concentration on the alginate-based films degradation rate. Ten-milligram samples were heated from 25 to 600 °C under

a nitrogen atmosphere at a flow rate of 50 mL min^{-1}. All experiments were conducted at 20 °C min^{-1} and the TG/DTG curves were recorded.

X-ray Diffraction (XRD)

X-ray diffraction analysis was performed using an X-ray analyzer (X'Pert-MPD, Philips, Almelo, Netherlands), using Cu Kα radiation (1.54056 Å) at a scan rate of 0.033333°/s (step = 0.04° and time per step = 1.2 s), with an acceleration voltage of 40 kV and an applied current of 40 mA, ranging from 5 to 60°.

Thickness

The average thicknesses of the films were measured using a digital electronic micrometer (Mitutoyo Co., Kawasaki-Shi, Japan), with a resolution of 0.1 µm. Measurements were performed at five random locations from five specimens from the same film formulation (ISO-4593, 1993).

Mechanical Properties

The samples were cut to a width of 15 mm using high-precision equipment (RDS-100-C, ChemInstruments, Fairfield, OH, USA). They were then conditioned for 48 h at 23 ± 2 °C and 50 ± 5% RH. The mechanical properties of tensile strength (MPa), elongation at break (%), and modulus of elasticity (MPa) were determined using a universal testing machine (Instron, 5966-E2, Norwood, MA, USA). The tests were performed with a 100-N load cell, at a speed of 12 mm min^{-1} and a distance of 50 mm. All tests were carried out with five repetitions (ASTM-D882, 2018).

Moisture Content

The moisture content (*MC*) of the films was evaluated by gravimetric method. The initial masses of the film samples were determined using an analytical balance (Mettler Toledo, Columbus, OH, USA) with a resolution of 10^{-4} g. The films were then heated to 105 °C for 24 h in an oven (Ethik Technology). After cooling the samples, the final masses were recorded. The *MC* values (%) were determined using four repetitions for each film sample analyzed, according to Eq. (1):

$$MC = \frac{w_i - w_f}{w_i} \times 100\% \quad (1)$$

where w_i and w_f are the initial and final masses of the samples, respectively.

Water Vapor Transmission Rate (WVTR)

For all film samples, water vapor transmission rate (WVTR) values were determined using the gravimetric method. Capsules with a permeation area of 50 cm^2 and an analytical balance (Mettler Toledo) with a 10^{-4} g resolution were used, with the tests carried out at 25 °C and 75% RH in an air-conditioning chamber (Weiss Technik, Reiskirchen, Germany), with anhydrous calcium chloride desiccant. The WVTR (g m^{-2} d^{-1}) was determined using four repetitions from the slope of the curve "mass vs. time" (ASTM-E96/E96M, 2016).

Light Transmission

The light transmission of the film samples was measured in the broad wavelength range (from UV to visible) between 200 and 800 nm, using a double-beam UV–visible spectrophotometer (Specord 210, Analytik Jena GmbH, Jena, Germany), with a scanning speed of 120 nm min^{-1} (ASTM-E-1348, 2015). The tests were performed in triplicate.

Statistical Analysis

The results were statistically analyzed using an analysis of variance (ANOVA) and the Tukey test to compare the average values. Differences were considered to be statistically significant if $p < 0.05$.

Results and Discussion

Surface Morphology

Scanning electron microscopy (SEM) can reveal the dispersion conditions of each component in a polymer blend and also the state of the interface phases. The SEM images of the sodium alginate blend films incorporating different loads of hydrolyzed collagen are presented in Fig. 1. It is possible to observe the microstructural changes in the samples due to the addition of hydrolyzed collagen in the top and cross-sectional topographies of the films. The surface and cross-sectional micrographs of the sodium alginate control films displayed a smoother and flatter morphology, compared to the blended films, presenting slight irregularities at a magnification of 1000×. These control images were similar to those typically reported in the literature (Aloui et al., 2021; Yerramathi et al., 2021). However, the addition of hydrolyzed collagen at concentrations from 10 to 30% produced noticeable (at magnification of 1000×) irregularities and cracks on the blended films, disrupting the continuity of the alginate matrix.

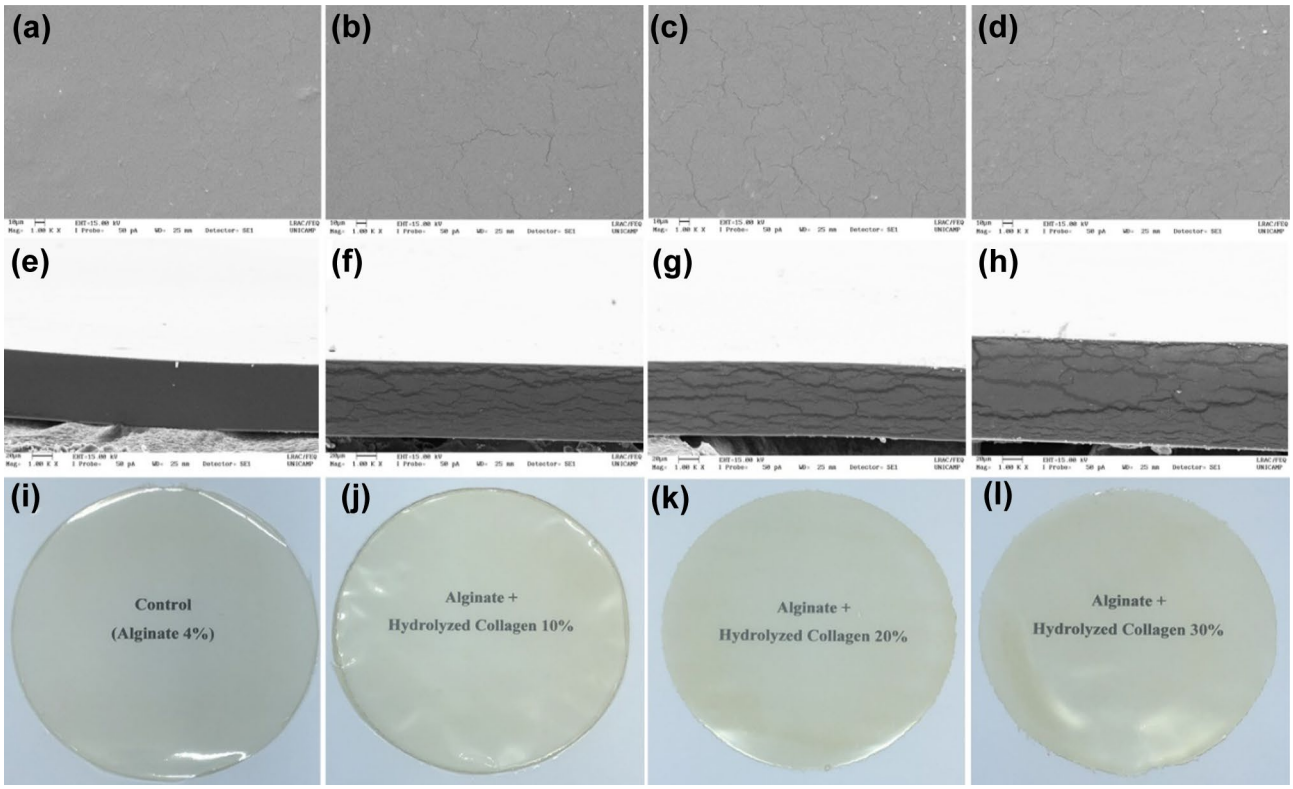

Fig. 1 Scanning electron micrography of sodium alginate films with different percentages of hydrolyzed collagen showing the top (**a**, **b**, **c**, **d**) and cross-sectional (**e**, **f**, **g**, **h**) views, along with images of the films with no magnification (**i**, **j**, **k**, **l**)

FTIR Spectroscopy

Infrared spectroscopy can be employed to determine the functional groups of biopolymers and the possible intermolecular interactions between them. For this, the shifting of the chemical bonds' absorption peaks is identified on the material spectra. The impact of hydrolyzed collagen addition on the shifting of characteristic bonds of sodium alginate films is displayed in Fig. 2.

The typical functional groups of SA were found in all films analyzed (Fig. 2). For the control film, the peaks at wavenumbers around 3344 and 2925 cm^{-1} are characteristic of –OH stretching and a weak aliphatic C–H stretching band, respectively. The sharp peak observed at 1040 cm^{-1} can be attributed to the elongation of the C–O groups (Pereira et al., 2011). Asymmetric and symmetric stretching vibrations of COO^- have been reported at the wavenumbers, 1606 and 1406 cm^{-1}, respectively (Santos et al., 2020). Because of the low HC loads, the characteristic bands of amides were noticed in the blends only with very low intensity, at approximately 1548 cm^{-1}. This may be related to signals overlap referring to the stretching vibrations of the carbonyl groups (C = O), which are present in both SA and HC.

The transmittance of the –OH group band increased by the addition of hydrolyzed collagen (from approximately 85 to 88%, for SA and SA/HC30%, respectively). There was also a slight shift of the spectrum to lower wavelength regions (from 3344 to 3303 cm^{-1} for SA and SA/HC30%, respectively), indicating that hydrogen bonds had been formed between the polymers in the blended films. The same behavior was also exhibited for the C–O (1040 cm^{-1}) and COO^- (1606 cm^{-1}) group vibrations, confirming the hypothesis of the existence of intermolecular interactions between polymeric matrices. However, it was found that these interactions were not as high as expected when low HC loads were added.

Thermogravimetric Analysis

Thermal stability is a crucial parameter for the industrial processing and applications of blended films. The results from the thermogravimetric characterization of the sodium alginate films blended with hydrolyzed collagen are shown in Fig. 3. The curves show the mass loss of the samples throughout their thermal decomposition (Fig. 3a) and their associated derivatives (Fig. 3b). This showed that the degradation of all films tested occurred as two different thermal events, which is typical for sodium alginate-based films (Aloui et al., 2021; Liu et al., 2017).

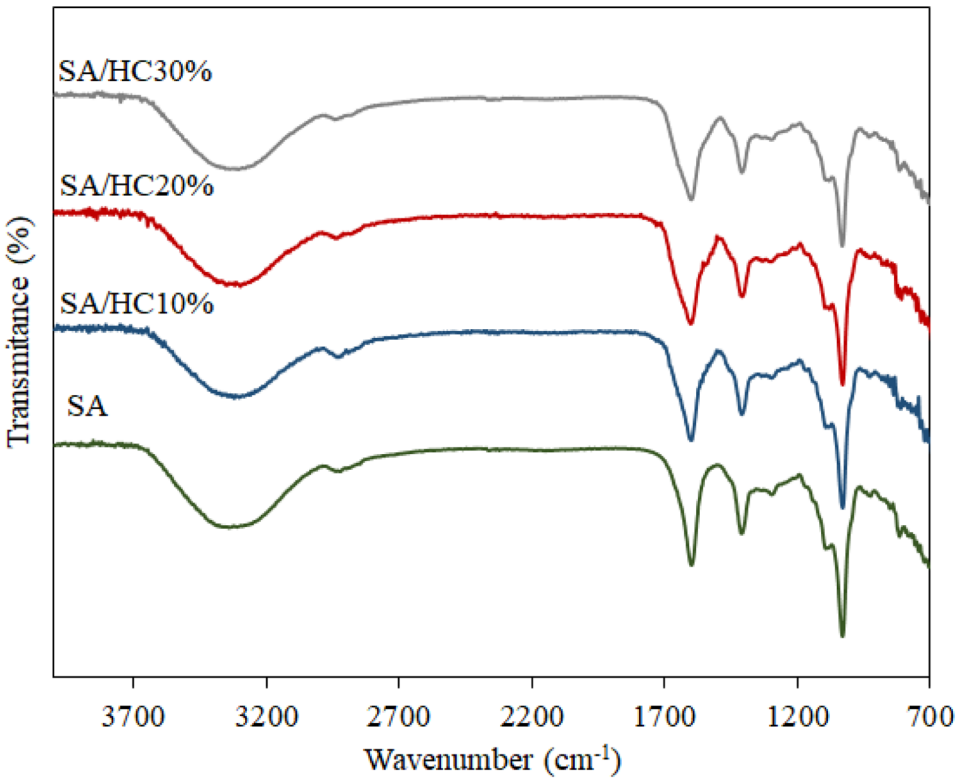

Fig. 2 FTIR spectra of sodium alginate films with hydrolyzed collagen

For all formulations studied, the first thermal event occurred before 100 °C, which is associated with the evaporation of free water from the films. Consecutively, the second thermal event was attributed to the decomposition of sodium alginate constituents (Liu et al., 2017). Table 1 displays the initial degradation (T_{onset}) and maximum decomposition (T_{max}) temperatures for both thermal events registered on the thermograms. T_{onset} and T_{max} for the SA control film were 214.37 and 226.51 °C, respectively. These results are similar to those found by Aloui et al. (Aloui et al., 2021).

The incorporation of hydrolyzed collagen in the sodium alginate films increased the blend's T_{onset} and T_{max} values (Table 1) compared with the control SA thermal behavior, especially for the composition of SA/HC30%. This behavior may be attributed to increasing the extent of hydrogen bonding upon increasing the HC content. Furthermore, the HC

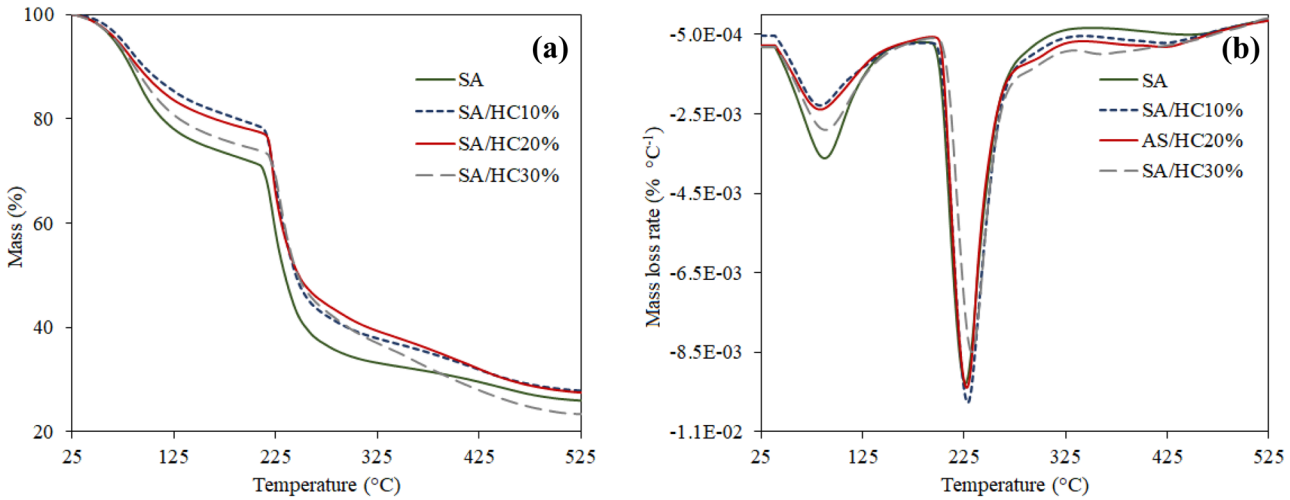

Fig. 3 TGA (**a**) and DTGA (**b**) curves of sodium alginate films with hydrolyzed collagen

Table 1 Initial degradation (T_{onset}) and maximum decomposition (T_{max}) temperatures of sodium alginate films with hydrolyzed collagen

Sample	First thermal event (°C)		Second thermal event (°C)	
	T_{onset}	T_{max}	T_{onset}	T_{max}
SA	59.45	87.83	214.37	226.51
SA/HC10%	54.46	83.30	215.31	228.56
SA/HC20%	53.47	82.45	216.96	227.02
SA/HC30%	57.12	88.00	220.61	232.89

load decreased the average mass loss rate (Fig. 3a) of the films, suggesting that adding HC contributes to the integrity of the films at higher temperatures. Even though low concentrations of HC were used, it is confirmed that its incorporation in alginate films clearly improves its thermal stability.

The thermal degradation of hydrolyzed collagen occurs over a range close to that previously identified for sodium alginate control films (Sadeghi & Hosseinzadeh, 2013). Similar behavior was observed in a study aiming to enhance the stability and mechanical strength of sodium alginate composite films with graphene oxide, ammonia functionalized graphene oxide, and triethoxylpropylaminosilane functionalized silica (Liu et al., 2017). It is important to note that the results reported in the present study were superior to those published by Aloui et al., who observed a decrease in T_{onset} and T_{max} of sodium alginate films with added gallnut extract (Aloui et al., 2021). The authors also disclosed that incorporating the gallnut extract in the SA matrix increased the average mass loss rate of the films.

X-ray Diffraction

Crystallinity, the molecular ordering in a material structure, is a critical characteristic that widely affects the mechanical properties of polymers, such as yield stress, elastic modulus, and impact resistance (Rodrigues & Druzian, 2018). In order to investigate this characteristic, Fig. 4 shows the XRD spectra of the blended films produced in the present study as well as those of the SA control. It is possible to observe (Fig. 4) the diffraction peaks at 2θ for all films assessed and their intensity variations due to the different formulations.

The materials analyzed exhibited semi-crystalline structures, predominantly amorphous. The XRD spectra of the control SA sample showed a small peak at 2θ ≈ 13° and a broad diffraction peak at 2θ ≈ 20°, which indicates a low crystallinity (Bhagyaraj & Krupa, 2020). A similar profile was observed for all blended films. However, there was a slight increase in the intensity of the crystalline peaks with the addition of hydrolyzed collagen. This phenomenon suggests the establishment of intermolecular interactions between sodium alginate and hydrolyzed collagen, making the blended films a little more crystalline than the SA control. The presence of such interactions was confirmed in

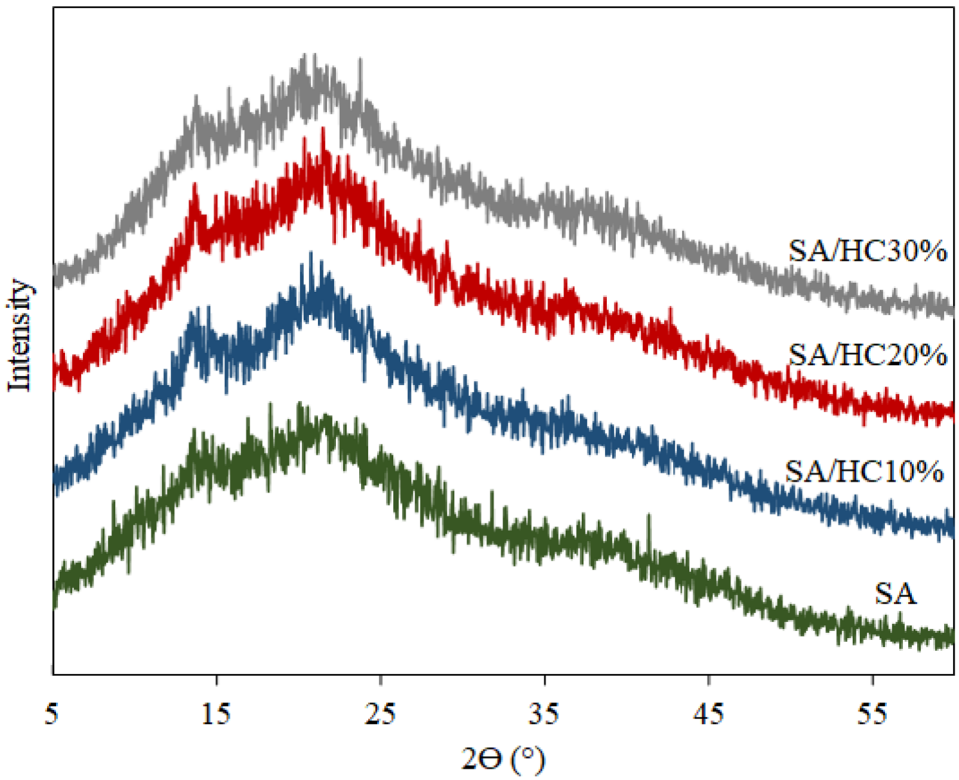

Fig. 4 XRD pattern of sodium alginate films with hydrolyzed collagen

the FTIR spectra (Fig. 2) by the shift in the vibration of the functional groups in the blended films and may also be associated with the increase in the thermal stability of the alginate-based films as the hydrolyzed collagen load increased.

Thickness and Mechanical Properties

According to the thickness results (Table 2), the SA film (control) was the thinnest (83.3 ± 10.2 µm), while the SA/HC20% film was the thickest (116.6 ± 22.5 µm). In addition, films with 10 and 30% HC were approximately 100 µm thick, significantly different ($p < 0.05$) from the SA and SA/HC20% films. These results indicate that the thickness of the films was influenced by the interaction between SA and HC, and can be explained by the alignment of the CH peptide chains in the polymeric matrix, resulting in a lower degree of film compaction and, consequently, greater thickness in relation to the control sample (Ahmad et al., 2016; Ocak, 2018). It is also important to note that variations in the film thickness depend on the composition and film-forming solution, the nature of the film components, as well as the preparation and drying conditions (Ahmad et al., 2012). Finally, the higher thickness of films with 20% HC in relation to the films with 30% HC may be due to variations along the matrix that come from the casting method used in the production of the films.

The mechanical properties of packaging materials are of great importance for maintaining their integrity and stability during handling, storage, and transportation (Marangoni Júnior et al., 2020b, c; Shahbazi, 2017). The characteristics of tensile strength (TS), elongation at break (EB), and modulus of elasticity (ME) of the SA/HC films are shown in Table 2. The tensile strength varied between 15.5 ± 2.2 and 20.4 ± 4.5 MPa and showed no significant difference between the different formulations. These results were different from those found for cellulose-based films whose tensile strength was reduced by the addition of hydrolyzed collagen (Pei et al., 2013). Therefore, in this present study, the addition of hydrolyzed collagen did not have the same negative effect on the TS of the SA-based films.

Regarding the elongation at break, the values for SA and SA/HC10% films were not significantly different ($p > 0.05$). The film with 10% of HC exhibited the highest average value (18.9%). Conversely, the EB of the SA/HC20% and SA/HC30% films were significantly reduced ($p < 0.05$) compared with that of the SA/HC10% film. In this sense, the elongation at break tends to decrease continuously as the HC content increases. This behavior was also observed for polyethylene films with added HC (Dascălu et al., 2005; Senra & Marques, 2020). It is important to note that the addition of higher HC loads negatively impacted the morphology of the films, as discussed in the "Surface Morphology" section. This significant reduction in film elongation may also be correlated with the cracks observed in the fracture micrographs of the SA/HC films (Fig. 1), since these defects can act as stress concentrators during the mechanical test, providing rapid crack propagation and consequently an early failure.

In addition, the modulus of elasticity of the SA/HC10% and SA/HC30% films did not differ significantly from the control (SA), with values of 619.9 ± 77.9 and 885.9 ± 104.0 MPa, respectively. However, although a significant increase ($p < 0.05$) in EM was observed for the SA/HC20% film, but it was not significantly different ($p > 0.05$) to that of the SA/HC30% film. The increase in stiffness (high EM) may have occurred due to more intense intermolecular interactions with larger proportions of HC in the blends. On the other hand, the brittleness (low EB values) of the films may be associated with the fact that HC molecules with low molar masses were added, which cannot significantly contribute to the plastic deformation of the material as a whole. In addition, the defects (cracks) observed in the microstructure may also have contributed to this large reduction in EB. In general, the 10% HC films underwent no changes in the mechanical properties evaluated in relation to the control and exhibited a better EB result than the other films with added HC. Therefore, this formulation (SA/HC10%) could be explored in future studies aiming at the incorporation of other materials, such as nanoparticles, for example, in order to achieve better mechanical properties.

Table 2 Thickness and mechanical properties of sodium alginate films with hydrolyzed collagen

Sample	Thickness (µm)	Tensile strength (MPa)	Elongation at break (%)	Modulus of elasticity (MPa)
SA	83.3 ± 10.2^{c}	18.4 ± 3.1^{a}	11.1 ± 7.4^{ab}	762.4 ± 117.0^{bc}
SA/HC10%	101.0 ± 13.4^{b}	20.4 ± 4.5^{a}	18.9 ± 7.6^{a}	619.9 ± 77.9^{c}
SA/HC20%	116.6 ± 22.5^{a}	19.5 ± 1.8^{a}	6.2 ± 2.2^{b}	957.1 ± 105.3^{a}
SA/HC30%	102.8 ± 13.6^{b}	15.5 ± 2.2^{a}	4.0 ± 2.4^{b}	885.8 ± 104.0^{ab}

The results are expressed as an average of five repetitions ± standard deviation

^{a,b,c}The means, followed by the same letter, in the column, do not differ at the 95% confidence level ($p > 0.05$)

Table 3 Moisture content and water vapor transmission rate of sodium alginate films with hydrolyzed collagen

Sample	Moisture content (%)	WVTR (g m^{-2} day^{-1})
SA	82.8 ± 0.2^{b}	1215.7 ± 71.0^{a}
SA/HC10%	82.9 ± 0.1^{b}	978.6 ± 78.3^{b}
SA/HC20%	84.7 ± 0.4^{a}	790.6 ± 121.0^{c}
SA/HC30%	84.9 ± 0.1^{a}	592.4 ± 52.2^{d}

The results are expressed as mean ± standard deviation

[a,b,c]The means, followed by the same letter, in the column, do not differ at the 95% confidence level ($p > 0.05$)

Moisture Content and Water Vapor Transmission Rate

The results on moisture content (*MC*) of the SA/HC blended films are shown in Table 3. The values were between 82.8 ± 0.2 and 84.9 ± 0.1%. *MC* values above 80% have also been found in the literature for SA-based films (Yerramathi et al., 2021). In addition, it was observed that the addition of 20 and 30% HC resulted in a significant increase ($p < 0.05$) in the *MC* compared with the control (SA) and the SA/HC10% films, which may be due the greater affinity of HC with water (Ahmad et al., 2016), or also because of an unsatisfactory drying time. In this sense, it is suggested that future studies should determine moisture sorption isotherms to investigate such interactions.

The water vapor barrier is an important property for evaluating the performance and the mass transfer mechanism of biopolymer-based films for applications such as food packaging, since this property has a direct influence on the shelf life of products (Ferreira et al., 2016; Marangoni Júnior et al., 2021c; de Morais Lima et al., 2017). In addition, polysaccharide-based films tend to have a low water vapor barrier due to their hydrophilic nature (Ferreira et al., 2016). The results of determining water vapor barrier properties are shown in Table 3. The WVTR of the SA films decreased significantly ($p < 0.05$) due to the increase in collagen content. These results are consistent with an increase in the thickness of the film due to the higher concentration of solids in the polymeric matrix. In addition, this behavior may be due to better integration of the film matrix, evidenced by a stronger intermolecular (polysaccharide-protein) interaction that modifies the micro-paths and delays the transfer of moisture through the film (Ahmad et al., 2012, 2016).

Light Barrier Properties

The characterization of light transmission is an important property for films based on biopolymers, since the exposure of foods to light may result in reactions which degrade nutrients. In addition, depending on the application, the packaging can act as a light barrier, delaying the photodegradation of food (Marangoni Júnior et al., 2020a,

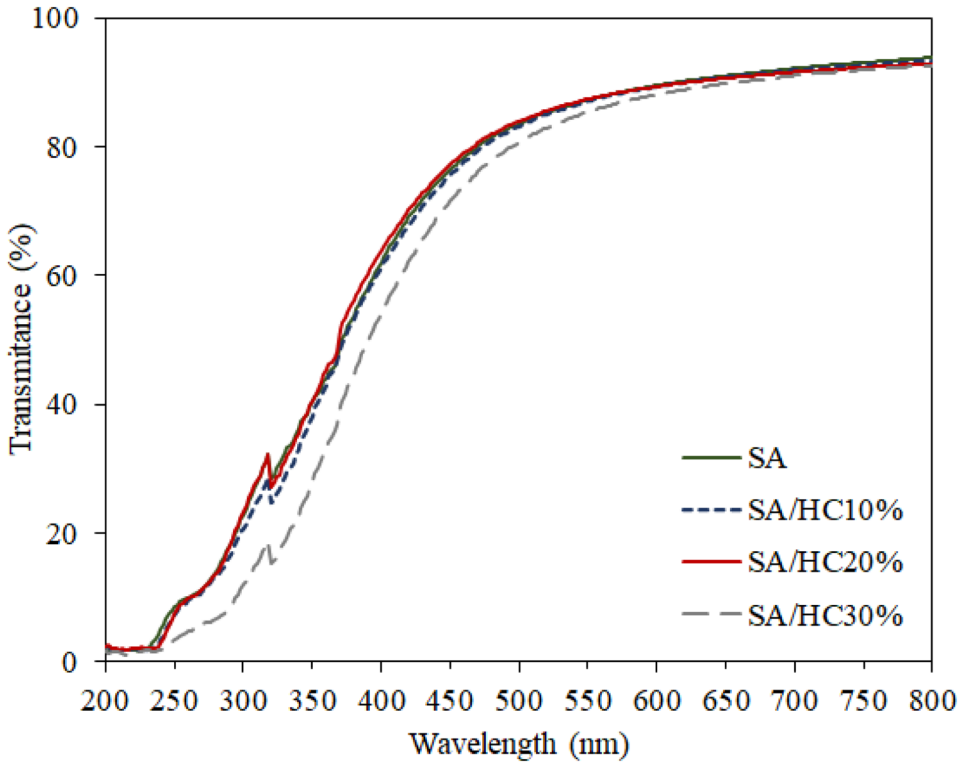

Fig. 5 Light transmission (%) of sodium alginate films with hydrolyzed collagen

d, 2021a). The light transmissions in the UV–visible range of SA films with different proportions of HC are shown in Fig. 5. In the 200–300 nm UV range, all films had a high light barrier (light transmission < 15%). However, light transmission gradually increased in the visible range of 300–800 nm, to approximately 90%. The light transmission profile of the SA, SA/HC10%, and SA/HC20% films was identical. However, for the SA/HC30% film the light transmission was slightly lower, both in the UV and in the visible range. This behavior may be due to the greater amount of solids present in the film. In addition, a higher concentration of HC in the film has been reported to result in an increase in aromatic amino acids, which are sensitive chromophores that can absorb light at wavelengths below 300 nm (Ahmad et al., 2016; Fakhreddin Hosseini et al., 2013; Guerrero et al., 2011; Jridi et al., 2014). Still in this context, the interaction between SA molecules with HC results in a more compact structure, which consequently can delay the transmission of light, as was observed for the SA/HC30% film.

Conclusions

In the present study, the sodium alginate/hydrolyzed collagen films were successfully developed and were visually attractive, with uniform coloring. SEM images showed the addition of hydrolyzed collagen led to a discontinuity in the polymeric matrix. However, this discontinuity did not adversely influence the tensile strength of the films. It was possible to conclude that intermolecular interactions had formed between sodium alginate and hydrolyzed collagen, based on the FT-IR spectra data, where the peak intensity of the groups –OH, C–O, and C–H decreased with the addition of hydrolyzed collagen and also from the increase in crystallinity based on the XRD results. In addition, the incorporation of hydrolyzed collagen increased the thermal stability of the sodium alginate films. The films became thicker as the hydrolyzed collagen concentration increased, positively impacting the WVTR of the films. As a general conclusion, a loading of 10% hydrolyzed collagen in sodium alginate-based films resulted in superior properties; therefore, this formulation is recommended for future research.

Acknowledgements The authors acknowledge the National Council for Scientific and Technological Development (CNPq).

Author Contribution Luís Marangoni Júnior: conceptualization; data curation; formal analysis; funding acquisition; investigation; methodology; project administration; resources; roles/writing—original draft; writing—review and editing. Plínio Ribeiro Rodrigues: data curation; investigation; roles/writing—original draft; writing—review and editing. Renan Garcia da Silva: formal analysis; investigation; writing—review and editing. Rosa Maria Vercelino Alves: conceptualization; data curation; formal analysis; funding acquisition; investigation; methodology; project administration; resources; supervision; writing—review and editing. Roniérik Pioli Vieira: conceptualization; data curation; formal analysis; funding acquisition; investigation; methodology; project administration; resources; supervision; roles/writing—original draft; writing—review and editing.

Funding This study was partly financed by the Coordination for the Improvement of Higher Education Personnel—Brazil (CAPES)—Financial Code 001.

Availability of Data and Material Data will be made available on request from the authors.

Declarations

Competing Interests The authors declare no competing interests.

References

Ahmad, M., Benjakul, S., Prodpran, T., & Agustini, T. W. (2012). Physico-mechanical and antimicrobial properties of gelatin film from the skin of unicorn leatherjacket incorporated with essential oils. *Food Hydrocolloids, 28,* 189–199. https://doi.org/10.1016/j.foodhyd.2011.12.003.

Ahmad, M., Nirmal, N. P., Danish, M., Chuprom, J., & Jafarzedeh, S. (2016). Characterisation of composite films fabricated from collagen/chitosan and collagen/soy protein isolate for food packaging applications. *RSC Advances, 6*, 82191–82204. https://doi.org/10.1039/c6ra13043g

Aloui, H., Deshmukh, A. R., Khomlaem, C., & Kim, B. S. (2021). Novel composite films based on sodium alginate and gallnut extract with enhanced antioxidant, antimicrobial, barrier and mechanical properties. *Food Hydrocolloids, 113,* 106508. https://doi.org/10.1016/j.foodhyd.2020.106508

ASTM-D882. (2018). Standard test method for tensile properties of thin plastic sheeting. West Conshohocken, 12p.

ASTM-E96/E96M. (2016). Standard test methods for water vapor transmission of materials, West Conshohocken, 14p.

ASTM-E-1348. (2015). Standard test method for transmittance and color by spectrophotometry using hemispherical geometry. West Conshohocken, 3p.

Bhagyaraj, S., & Krupa, I. (2020). Alginate-mediated synthesis of hetero-shaped silver nanoparticles and their hydrogen peroxide sensing ability. *Molecules, 25*, 435. https://doi.org/10.3390/molecules25030435

Berti, S., Jagus, R. J., & Flores, S. K. (2021). Effect of rice bran addition on physical properties of antimicrobial biocomposite films based on starch. *Food and Bioprocess Technology*. https://doi.org/10.1007/s11947-021-02669-0

Cazón, P., Velazquez, G., Ramírez, J. A., & Vázquez, M. (2017). Polysaccharide-based films and coatings for food packaging: A review. *Food Hydrocolloids, 68,* 136–148. https://doi.org/10.1016/j.foodhyd.2016.09.009.

Dascălu, M. C., Vasile, C., Silvestre, C., & Pascu, M. (2005). On the compatibility of low density polyethylene/hydrolyzed collagen blends. II: New compatibilizers. *European Polymer Journal*, *41*, 1391–1402. https://doi.org/10.1016/j.eurpolymj.2004.12.005

da Silva Pereira, G. V., da Silva Pereira, G. V., Xavier Neves, E. M. P., Albuquerque, G. A., de Arimatéia Rodrigues do Rêgo, J.,

Cardoso, D. N. P., do Socorro Barros Brasil, D., & Joele, M. R. S. P. (2021). Effect of the mixture of polymers on the rheological and technological properties of composite films of acoupa weakfish (Cynoscion acoupa) and cassava starch (Manihot esculenta C.). *Food Bioprocess Technology 14*, 1199–1215. https://doi.org/10.1007/s11947-021-02622-1

de Morais Lima, M., Bianchini, D., Guerra Dias, A., da Rosa Zavareze, E., Prentice, C., & da Silveira Moreira, A. (2017). Biodegradable films based on chitosan, xanthan gum, and fish protein hydrolysate. *Journal of Applied Polymer Science*, *134*, 1–9. https://doi.org/10.1002/app.44899

de Oliveira Filho, J. G., Braga, A. R. C., de Oliveira, B. R., Gomes, F. P., Moreira, V. L., Pereira, V. A. C., & Egea, M. B. (2021). The potential of anthocyanins in smart, active, and bioactive eco-friendly polymer-based films: A review. *Food Research International, 142*, 110202. https://doi.org/10.1016/j.foodres.2021.110202

Denis, A., Brambati, N., Dessauvages, B., Guedj, S., Ridoux, C., Meffre, N., & Autier, C. (2008). Molecular weight determination of hydrolyzed collagens. *Food Hydrocolloids*, *22,* 989–994. https://doi.org/10.1016/j.foodhyd.2007.05.016

Fakhreddin Hosseini, S., Rezaei, M., Zandi, M., & Ghavi, F. F. (2013). Preparation and functional properties of fish gelatin-chitosan blend edible films. *Food Chemistry*, *136*, 1490–1495. https://doi.org/10.1016/j.foodchem.2012.09.081

Ferreira, A. R. V., Torres, C. A. V., Freitas, F., Sevrin, C., Grandfils, C., Reis, M. A. M., Alves, V. D., & Coelhoso, I. M. (2016). Development and characterization of bilayer films of FucoPol and chitosan. *Carbohydrate Polymers, 147*, 8–15. https://doi.org/10.1016/j.carbpol.2016.03.089

Gagliarini, N., Diosma, G., Piermaria, J., Garrote, G. L., & Abraham, A. G. (2019). Whey protein-kefiran films as driver of probiotics to the gut. *LWT - Food Science and Technology, 105,* 321–328. https://doi.org/10.1016/j.lwt.2019.02.023.

Garrido, T., Peñalba, M., de la Caba, K., & Guerrero, P. (2019). A more efficient process to develop protein films derived from agro-industrial by-products. *Food Hydrocolloids*, *86,* 11–17. https://doi.org/10.1016/j.foodhyd.2017.11.023

Gomez-Guillen, M. C., Gimenez, B., Lopez-Caballero, M. E., & Montero, M. P. (2011). Functional and bioactive properties of collagen and gelatin from alternative sources: A review. *Food Hydrocolloids, 25,* 1813–1827. https://doi.org/10.1016/j.foodhyd.2011.02.007.

Gómez-Guillén, M. C., Pérez-Mateos, M., Gómez-Estaca, J., López-Caballero, E., Giménez, B., & Montero, P. (2009). Fish gelatin: A renewable material for developing active biodegradable films. *Trends in Food Science and Technology 20*, 3–16. https://doi.org/10.1016/j.tifs.2008.10.002

Guerrero, P., Nur Hanani, Z. A., Kerry, J. P., & De La Caba, K. (2011). Characterization of soy protein-based films prepared with acids and oils by compression. *Journal of Food Engineering*, *107*, 41–49. https://doi.org/10.1016/j.jfoodeng.2011.06.003

ISO-4593. (1993). Plastics: Film and sheeting determination of thickness by mechanical scanning. Switzerland, 2p.

Ito, N., Seki, S., & Ueda, F. (2018). Effects of composite supplement containing collagen peptide and ornithine on skin conditions and plasma IGF-1 levels—A randomized, double-blind, placebo-controlled trial. *Marine Drugs*, *16.* https://doi.org/10.3390/md16120482

Jamróz, E., Kopel, P., Juszczak, L., Kawecka, A., Bytesnikova, Z., Milosavljević, V., et al. (2018). Development and characterisation of furcellaran-gelatin films containing SeNPs and AgNPs that have antimicrobial activity. *Food Hydrocolloids, 83,* 9–16. https://doi.org/10.1016/j.foodhyd.2018.04.028.

Jridi, M., Hajji, S., Ben Ayed, H., Lassoued, I., Mbarek, A., Kammoun, M., Souissi, N., & Nasri, M. (2014). Physical, structural, antioxidant and antimicrobial properties of gelatin-chitosan composite edible films. *International Journal of Biological Macromolecules*, *67*, 373–379. https://doi.org/10.1016/j.ijbiomac.2014.03.054

Khashayary, S., & Aarabi, A. (2021). Evaluation of physico-mechanical and antifungal properties of gluten-based film incorporated with vanillin, salicylic acid, and montmorillonite (Cloisite 15A). *Food and Bioprocess Technology, 14*, 665–678. https://doi.org/10.1007/s11947-021-02598-y

León-López, A., Morales-Peñaloza, A., Martínez-Juárez, V. M., Vargas-Torres, A., Zeugolis, D. I., & Aguirre-Álvarez, G. (2019). Hydrolyzed collagen—Sources and applications. *Molecules*, *24.* https://doi.org/10.3390/molecules24224031

Liu, S., Li, Y., & Li, L. (2017). Enhanced stability and mechanical strength of sodium alginate composite films. *Carbohydrate Polymers, 160*, 62–70. https://doi.org/10.1016/j.carbpol.2016.12.048

Lupu, M., Gradisteanu Pircalabioru, G., Chifiriuc, M., Albulescu, R., & Tanase, C. (2020). Beneficial effects of food supplements based on hydrolyzed collagen for skin care (review). *Experimental and Therapeutic Medicine*, *20,* 12–17. https://doi.org/10.3892/etm.2019.8342

Mahmoud, M. E., Saleh, M. M., Zaki, M. M., & Nabil, G. M. (2020). A sustainable nanocomposite for removal of heavy metals from water based on crosslinked sodium alginate with iron oxide waste material from steel industry. *Journal of Environmental Chemical Engineering*, *8,* 104015. https://doi.org/10.1016/j.jece.2020.104015

Marangoni Júnior, L., Alves, R. M. V., Moreira, C. Q., Cristianini, M., Padula, M., & Anjos, C. A. R. (2020a). High-pressure processing effects on the barrier properties of flexible packaging materials. *Journal of Food Processing and Preservation*,. https://doi.org/10.1111/jfpp.14865

Marangoni Júnior, L., Cristianini, M., & Anjos, C. A. R. (2020b). Packaging aspects for processing and quality of foods treated by pulsed light. *Journal of Food Processing and Preservation*, *44*, 1–14. https://doi.org/10.1111/jfpp.14902

Marangoni Júnior, L., De Oliveira, L. M., Bócoli, P. F. J., Cristianini, M., Padula, M., & Anjos, C. A. R. (2020c). Morphological, thermal and mechanical properties of polyamide and ethylene vinyl alcohol multilayer flexible packaging after high-pressure processing. *Journal of Food Engineering*, *276*. https://doi.org/10.1016/j.jfoodeng.2020.109913

Marangoni Júnior, L., Vieira, R. P., & Anjos, C. A. R. (2020d). Kefiran-based films: Fundamental concepts, formulation strategies and properties. *Carbohydrate Polymer, 246,* 116609. https://doi.org/10.1016/j.carbpol.2020.116609

Marangoni Júnior, L., da Silva, R. G., Anjos, C. A. R., Vieira, R. P., & Alves, R. M. V. (2021a). Effect of low concentrations of SiO2 nanoparticles on the physical and chemical properties of sodium alginate-based films. *Carbohydrate Polymer*, *269*, 118286. https://doi.org/10.1016/j.carbpol.2021.118286

Marangoni Júnior, L., da Silva, R. G., Vieira, R. P., & Alves, R. M. V. (2021b). Water vapor sorption and permeability of sustainable alginate/collagen/SiO2 composite films. *LWT*, *152*, 112261. https://doi.org/10.1016/j.lwt.2021.112261

Marangoni Júnior, L., Vieira, R. P., Jamróz, E., & Anjos, C. A. R. (2021c). Furcellaran: An innovative biopolymer in the production of films and coatings. *Carbohydrates Polymer, 252*, 117221. https://doi.org/10.1016/j.carbpol.2020.117221

Motedayen, A. A., Khodaiyan, F., & Salehi, E. A. (2013). Development and characterisation of composite films made of kefiran and starch. *Food Chemistry, 136*, 1231–1238. https://doi.org/10.1016/j.foodchem.2012.08.073

Ocak, B. (2018). Film-forming ability of collagen hydrolysate extracted from leather solid wastes with chitosan. *Environmental Science and Pollution Research, 25*, 4643–4655. https://doi.org/10.1007/s11356-017-0843-z

Pei, Y., Yang, J., Liu, P., Xu, M., Zhang, X., & Zhang, L. (2013). Fabrication, properties and bioapplications of cellulose/collagen hydrolysate composite films. *Carbohydrate Polymers, 92*, 1752–1760. https://doi.org/10.1016/j.carbpol.2012.11.029

Pereira, R., Tojeira, A., Vaz, D. C., Mendes, A., & Bártolo, P. (2011). Preparation and characterization of films based on alginate and aloe vera. *International Journal of Polymer Analysis and Characterization, 16*, 449–464. https://doi.org/10.1080/1023666X.2011.599923

Rahmani, B., Hosseini, H., Khani, M., Farhoodi, M., Honarvar, Z., Feizollahi, E., Shokri, B., & Shojaee-Aliabadi, S. (2017). Development and characterisation of chitosan or alginate-coated low density polyethylene films containing Satureja hortensis extract. *International Journal of Biological Macromolecules*, *105*, 121–130. https://doi.org/10.1016/j.ijbiomac.2017.07.002

Ramadass, S. K., Perumal, S., Gopinath, A., Nisal, A., Subramanian, S., & Madhan, B. (2014). Sol–gel assisted fabrication of collagen hydrolysate composite scaffold: A novel therapeutic alternative to the traditional collagen scaffold. *ACS Applied Materials & Interfaces, 6*, 15015–15025. https://doi.org/10.1021/am502948g

Reyes-Avalos, M. C., Femenia, A., Minjares-Fuentes, R., Contreras-Esquivel, J. C., Aguilar-González, C. N., Esparza-Rivera, J. R., & Meza-Velázquez, J. A. (2016). Improvement of the quality and the shelf life of figs (Ficus carica) using an alginate–chitosan edible film. *Food and Bioprocess Technology, 9*, 2114–2124. https://doi.org/10.1007/s11947-016-1796-9

Ribeiro, A. M., Estevinho, B. N., & Rocha, F. (2021). Preparation and incorporation of functional ingredients in edible films and coatings. *Food and Bioprocess Technology, 14*, 209–231. https://doi.org/10.1007/s11947-020-02528-4

Rodrigues, P. R., & Druzian, J. I. (2018). Impact of different bacterial strains on the production, composition, and properties of novel polyhydroxyalkanoates using crude palm oil as substrate. *Chemical and Biochemical Engineering Quarterly*, *32*, 141–150. https://doi.org/10.15255/CABEQ.2017.1207

Sadeghi, M., & Hosseinzadeh, H. (2013). Synthesis and properties of collagen-g-poly(sodium acrylate-co-2-hydroxyethylacrylate) superabsorbent hydrogels, Brazilian. *Journal of Chemical Engineering, 30*, 379–389. https://doi.org/10.1590/S0104-66322013000200015

Santos, N. L., de O. Ragazzo, G., Cerri, B. C., Soares, M. R., Kieckbusch, T. G., & da Silva, M. A. (2020). Physicochemical properties of konjac glucomannan/alginate films enriched with sugarcane vinasse intended for mulching applications. *International Journal of Biological Macromolecules*, *165*, 1717–1726. https://doi.org/10.1016/j.ijbiomac.2020.10.049

Seggiani, M., Gigante, V., Cinelli, P., Coltelli, M. B., Sandroni, M., Anguillesi, I., & Lazzeri, A. (2019). Processing and mechanical performances of poly(butylene succinate–co–adipate) (PBSA) and raw hydrolyzed collagen (HC) thermoplastic blends. *Polymer Testing*, *77,* 105900. https://doi.org/10.1016/j.polymertesting.2019.105900

Senra, M. R., & Marques, M. D. F. V. (2020). Thermal and mechanical behavior of ultra-high molecular weight polyethylene/collagen blends. *Journal of the Mechanical Behavior of Biomedical Materials*, *103*. https://doi.org/10.1016/j.jmbbm.2019.103577

Shahbazi, Y. (2017). The properties of chitosan and gelatin films incorporated with ethanolic red grape seed extract and Ziziphora clinopodioides essential oil as biodegradable materials for active food packaging. *International Journal of Biological Macromolecules, 99*, 746–753. https://doi.org/10.1016/j.ijbiomac.2017.03.065

Silvipriya, K. S., Krishna Kumar, K., Bhat, A. R., Dinesh Kumar, B., John, A., & Lakshmanan, P. (2015). Collagen: Animal sources and biomedical application. *Journal of Applied Pharmaceutical Science*, *5,* 123–127. https://doi.org/10.7324/JAPS.2015.50322

Uyen, N. T. T., Hamid, Z. A. A., Tram, N. X. T., & Ahmad, N. (2020). Fabrication of alginate microspheres for drug delivery: A review. *International Journal of Biological Macromolecules, 153,* 1035–1046. https://doi.org/10.1016/j.ijbiomac.2019.10.233

Venkatesan, J., Bhatnagar, I., Manivasagan, P., Kang, K. H., & Kim, S. K. (2015). Alginate composites for bone tissue engineering: A review. *International Journal of Biological Macromolecules*, *72*, 269–281. https://doi.org/10.1016/j.ijbiomac.2014.07.008

Vianna, T. C., Marinho, C. O., Júnior, L. M., Ibrahim, S. A., & Vieira, R. P. (2021). Essential oils as additives in active starch-based food packaging films: A review. *International Journal of Biological Macromolecules*. https://doi.org/10.1016/j.ijbiomac.2021.05.170

Yerramathi, B. B., Kola, M., Annem Muniraj, B., Aluru, R., Thirumanyam, M., & Zyryanov, G. V. (2021). Structural studies and bioactivity of sodium alginate edible films fabricated through ferulic acid crosslinking mechanism. *Journal of Food Engineering*, *301*, 110566. https://doi.org/10.1016/j.jfoodeng.2021.110566

Zanela, J., Casagrande, M., Radaelli, J. C., Dias, A. P., Wagner Júnior, A., Malfatti, C. R. M., & Yamashita, F. (2021). Active biodegradable packaging for foods containing Baccharis dracunculifolia leaf as natural antioxidant. *Food and Bioprocess Technology*, *14,* 1301–1310. https://doi.org/10.1007/s11947-021-02641-y

Zhang, G., Sun, A., Li, W., Liu, T., & Su, Z. (2006). Mass spectrometric analysis of enzymatic digestion of denatured collagen for identification of collagen type. *Journal of Chromatography A*, *1114,* 274–277. https://doi.org/10.1016/j.chroma.2006.03.039